Bioresource Technology 200 (2016) 666–679

Contents lists available at ScienceDirect

Bioresource Technology

journal homepage: www.elsevier.com/locate/biortech

Dynamic global sensitivity analysis in bioreactor networks for bioethanol production

M.P. Ochoa, V. Estrada *, J. Di Maggio, P.M. Hoch

Planta Piloto de Ingeniería Química, CONICET, 8000 Bahía Blanca, Argentina
Universidad Nacional del Sur, Departamento de Ingeniería Química, 8000 Bahía Blanca, Argentina

HIGHLIGHTS

- Dynamic global sensitivity analysis (DGSA) on bioethanol production systems.
- DGSA on lignocellulosic bioethanol production.
- DGSA first order and interactional indices profiles for bioreactor state variables.
- Model parameters ranking based on global sensitivity analysis.
- DGSA with Sobol's method implemented in differential–algebraic modeling environment.

ARTICLE INFO

Article history:
Received 5 August 2015
Received in revised form 17 October 2015
Accepted 20 October 2015
Available online 27 October 2015

Keywords:
Dynamic global sensitivity analysis
Bioreactor networks
Bioethanol production
Co-fermentation
DAE systems

ABSTRACT

Dynamic global sensitivity analysis (GSA) was performed for three different dynamic bioreactor models of increasing complexity: a fermenter for bioethanol production, a bioreactors network, where two types of bioreactors were considered: aerobic for biomass production and anaerobic for bioethanol production and a co-fermenter bioreactor, to identify the parameters that most contribute to uncertainty in model outputs. Sobol's method was used to calculate time profiles for sensitivity indices. Numerical results have shown the time-variant influence of uncertain parameters on model variables. Most influential model parameters have been determined. For the model of the bioethanol fermenter, μ_{max} (maximum growth rate) and K_s (half-saturation constant) are the parameters with largest contribution to model variables uncertainty; in the bioreactors network, the most influential parameter is $\mu_{max,1}$ (maximum growth rate in bioreactor 1); whereas λ (glucose-to-total sugars concentration ratio in the feed) is the most influential parameter over all model variables in the co-fermentation bioreactor.

1. Introduction

During the last decades, there has been growing interest in biofuels production to complement fossil fuels. In particular, ethanol production from renewable resources (bioethanol) can improve energy security, reduce carbon dioxide emissions, and decrease urban air pollution (Chen and Wang, 2010). Currently, blends of gasoline and bioethanol can be used by more than 80% of light-duty vehicles (Datta et al., 2011) and many countries have legislated the commercialization of gasoline blends with increasing bioethanol content. Fermenters constitute the heart of bioethanol plants and much effort has been devoted to improve microorganisms and operating conditions (Romaní et al., 2015). Corsano et al. (2004) designed an optimal bioreactor network for bioethanol production from glucose as a mixed integer nonlinear programming problem. Many authors have proposed models for bioethanol production bioreactors by co-fermentation, using hexoses and pentoses as feedstock, with different microorganisms. Krishnan et al. (1999) proposed a model from glucose and xylose, using an engineered strain of *Saccharomyces*. More recently, Moreno et al. (2013) proposed and calibrated a model for an engineered *Zymomonas mobilis*, taking into account inhibition by furfural and HMF.

Bioreactor models for batch and fed-batch processes are formulated as differential–algebraic equation systems that result from mass balances formulation for substrates, biomass and products, kinetic expressions, design equations, hydraulic equations, etc. They include several parameters, most of which are related to biochemical reaction kinetics and whose values are usually uncertain. State variable values can be greatly influenced by the uncertainty of model parameters. Furthermore, as parameters are usually determined by means of experiments, there can be considerable

* Corresponding author. Tel.: +54 02914861700.
E-mail address: vestrada@plapiqui.edu.ar (V. Estrada).

http://dx.doi.org/10.1016/j.biortech.2015.10.069
0960-8524/

Nomenclature

DV_i	volume of distillery vinasses added to bioreactor i, m^3
$FEED_i$	feed for bioreactor i, m^3
I_{noc}	mass of inoculum, kg
K_s	substrate saturation constant, 20 kg m^{-3}
K_j	saturation coefficient for cell growth for substrate j, g = 0.565, x = 3.4 kg m^{-3}
$K_{i,j}$	inhibition coefficient for cell growth for substrate j, g = 283.7, x = 18.1 kg m^{-3}
K'_j	saturation coefficient for bioethanol production for substrate j, g = 1.342, x = 3.4 kg m^{-3}
$K'_{i,j}$	inhibition coefficient for bioethanol production for substrate j, g = 4890, x = 81.3 kg m^{-3}
M_i	volume of molasses added to bioreactor i, m^3
P_i	product concentration in bioreactor i, kg m^{-3}
P_g	product concentration from glucose, kg m^{-3}
P_x	product concentration from xylose, kg m^{-3}
p_{maxj}	maximum bioethanol concentration for cell growth for substrate j, g = 95.4, x = 59.04 kg m^{-3}
p'_{maxj}	maximum bioethanol concentration for bioethanol production for substrate j, g = 103, x = 60.2 kg m^{-3}
S_i	substrate concentration in bioreactor i, kg m^{-3}
R_1	first bioreactor of the network
R_2	second bioreactor of the network
S_{i0}	initial substrate concentration in bioreactor i, kg m^{-3}
S_g	glucose concentration, kg m^{-3}
S_f	feed sugar concentration, kg m^{-3}
S_x	xylose concentration, kg m^{-3}
S_{DV}	total concentration of reducing sugars in distillery vinasses, kg m^{-3}
S_M	total concentration of reducing sugars in molasses, kg m^{-3}
t	operation time, h
TRSs	total reduced sugar
V_{inoc}	inoculum size, m^{-3}
V_i	unit size of bioreactor
X_i	biomass concentration in bioreactor i, kg m^{-3}
X_{deadi}	inactive biomass concentration in bioreactor i, kg m^{-3}
$x_{1,i}$	contribution fraction of TRSs of molasses in bioreactor i
$x_{2,i}$	contribution fraction of TRSs of distillery vinasses in bioreactor i
$Y_{x/s,i}$	biomass yield coefficient in bioreactor i, 2 = 0.124
$Y_{x/p}$	product yield coefficient, 0.23
$Y_{p/sj}$	yield coefficient for bioethanol on substrate j, g = 0.47, x = 0.4

Subscripts

g	glucose
i	number of bioreactor in the network
j	substrate
x	xylose

Superscripts

int	interactional index
tot	total index

Greek symbols

λ	glucose-to-total sugar concentration ratio in the feed, 0.65
μ_i	specific growth rate of biomass in bioreactor i, h^{-1}
$\mu_{max,i}$	maximum specific growth rate of biomass in bioreactor i, 1 = 0.5, 2 = 0.1 h^{-1}
$\mu_{max,j}$	maximum specific growth rate of biomass from substrate j, g = 0.662, x = 0.19 h^{-1}
$\nu_{max,j}$	maximum specific rate of product formation from substrate j, g = 2.005, x = 0.25 h^{-1}
ν_{dead}	biomass death rate, 0.02 h^{-1}
ϕ_j	power of bioethanol inhibition for cell growth from substrate j, g = 1.29, x = 1.036
φ_j	power of bioethanol inhibition for bioethanol production from substrate j, g = 1.42, x = 0.608
χ_g	glucose conversion
χ_x	xylose conversion

uncertainty in their final value. For this reason, it is important to identify the parameters to which model state variables are most sensitive, which is achieved in general by a sensitivity analysis (SA). Techniques for sensitivity analysis can be classified into local and global. Local methods concentrate on the local impact of factors on the model, usually carried out by computing partial derivatives of the output functions with respect to the input variables. It is a particular case of one-factor-at-a-time (OAT) approach, since when a factor is varied; all the others are held constant. Local methods are less helpful when SA is used to compare the effect of various factors on the output. It has been recognized (Cukier et al., 1973) in the literature for a number of years that when the model is nonlinear and various input variables are affected by uncertainties of different orders of magnitude, a GSA method should be used (Saltelli et al., 2008). Global sensitivity analysis techniques include Morris' method (Morris, 1991), Sobol's method (Sobol', 2001), Fourier's Test (FAST: Fourier Amplitude Sensitivity Test) (Cukier et al., 1973) and control variate technique (Kucherenko et al., 2015). Global techniques incorporate the influence of the whole range of variation and the form of the probability density function in the input. GSA method evaluates the effect of factor x_i while all others x_j, $j \neq i$, are varied as well. In contrast, the local perturbative approach is based on partial derivatives, the effect of variation of the input factor x_i when all other x_j, $j \neq i$, are kept constant at their nominal value. Additionally, when these techniques are applied in dynamic models, a temporal profile of the influence of the parameters can be obtained, which gives great insight on the importance of the parameters not only related to each other but also during the time horizon.

Global sensitivity analysis (GSA) has been applied on a few biological systems during the last decade. Di Maggio et al. (2010) have performed GSA on dynamic metabolic networks to determine the most influential parameters in intracellular biochemical reactions. GSA has also been applied dynamic bioreactor network (Ochoa and Hoch, 2011). In addition, Kent et al. (2013) have applied GSA to a selection of five signaling and metabolic models to study how results can change under increasing amounts of parameter uncertainty, concluding that random sampling may be the most suitable technique for GSA. Other example of GSA on a biological model has been presented by Román-Martínez et al. (2014) on the control of a wastewater treatment. More recently, Savvopoulos et al. (2015) carried out global sensitivity analysis on a mathematical model of *B* cell chronic lymphocytic leukemia (B-CLL) using the random sampling high dimensional mathematical representation (RS-HDMR) method in order to determine the most critical model parameters. Within ecological systems, Estrada and Diaz (2010) applied GSA to a complex water quality model, on more than 20 parameters in 30 differential and 60 algebraic equations.

A comprehensive review, analysis and categorization research of GSA methods and their applications in the field of hydrological modeling has been presented by Song et al. (2015).

Regarding biofuels production, GSA has been applied to steady state models. Three different methods, variance-based, moment-independent and entropy-based, have been applied to quantify the contribution of an individual uncertain parameter in the techno-economic assessments of biodiesel production (Tang et al., 2015). Todri et al. (2014) have used global sensitivity analysis in bioethanol production processes, replacing complex models with surrogate models. Muhaimin Samsudin and Mat Don (2015) have carried out Monte Carlo simulations on an oil palm trunk sap fermentation model to evaluate model uncertainty; however, to analyze parametric sensitivity, they have performed local sensitivity analysis by changing each parameter in ±10% and ±50%.

In this work, global sensitivity analysis on three different dynamic models of bioethanol producing bioreactors of increasing complexity was carried out. They include a bioethanol fermenter based on glucose; a two-bioreactor network for bioethanol production based on glucose and a co-fermentation bioreactor based on glucose and xylose for bioethanol production. The models and the GSA methodology were implemented in an equation oriented environment with a differential algebraic equation solver in gPROMS (PSEnterprise Ltd., 2014). The implemented GSA strategy is variance-based (Sobol', 1993) and allows the determination and classification of model parameters, according to their sensitivity indices. Temporal profiles of first order effect sensitivity indices and those due to interactions with other model parameters have been calculated for parameters in the three studied bioreactor models. Numerical results show that the higher computational cost of global sensitivity analysis is thoroughly justified in complex nonlinear models describing bioreactors, where not only first order effects due to each parameter can be captured, but also due to interaction with other model parameters. In the most complex analyzed case, the co-fermentation bioreactor, GSA allows determining that parameters like yield and maximum growth rate are more influential through their effects due to interactions with other parameters than due to first order effects along the entire time horizon. A proper knowledge of model parameters influence on state variables has allowed their classification and provides useful information for parameter estimation in bioreactor and bioreactor network models.

2. Methodology

2.1. Mathematical model

In this work, three different bioreactor models of increasing complexity were proposed. Model (*i*) is a biomass-ethanol producing fermenter, model (*ii*) is a bioreactor network used in the production of bioethanol from molasses sugar and vinasses distillates in two stages (yeast growth and bioethanol production); and model (*iii*) is an bioethanol co-fermentation bioreactor based on glucose and xylose with a genetically modified yeast. The proposed models comprise a set of differential and algebraic equations that describe mass balances in fermenters, as well as algebraic kinetic expressions and connection constraints in the network case.

Kinetic models (*i*) and (*ii*) were the basis of dynamic optimization of fermentation processes with design purposes (Corsano et al., 2006, 2011; Albernas-Carvajal et al., 2014). Kinetic model (*iii*) was implemented in a dynamic modeling framework for the assessment of different operational scenarios by Morales-Rodriguez et al. (2011a). In addition, the co-fermentation model was also applied with optimal design (Chen and Wang, 2010) and with multi-objective optimization purposes (Sharma and Rangaiah, 2013).

2.1.1. Model (i)

In this case, a fermentation process in which sub-products and residues of a food process are used as substrates, such as molasses diluted with water and distillery vinasses, was considered (Corsano et al., 2004). Fig. 1(a) shows the scheme for this process. Molasses are by-products obtained from a sugar plant crystallizer,

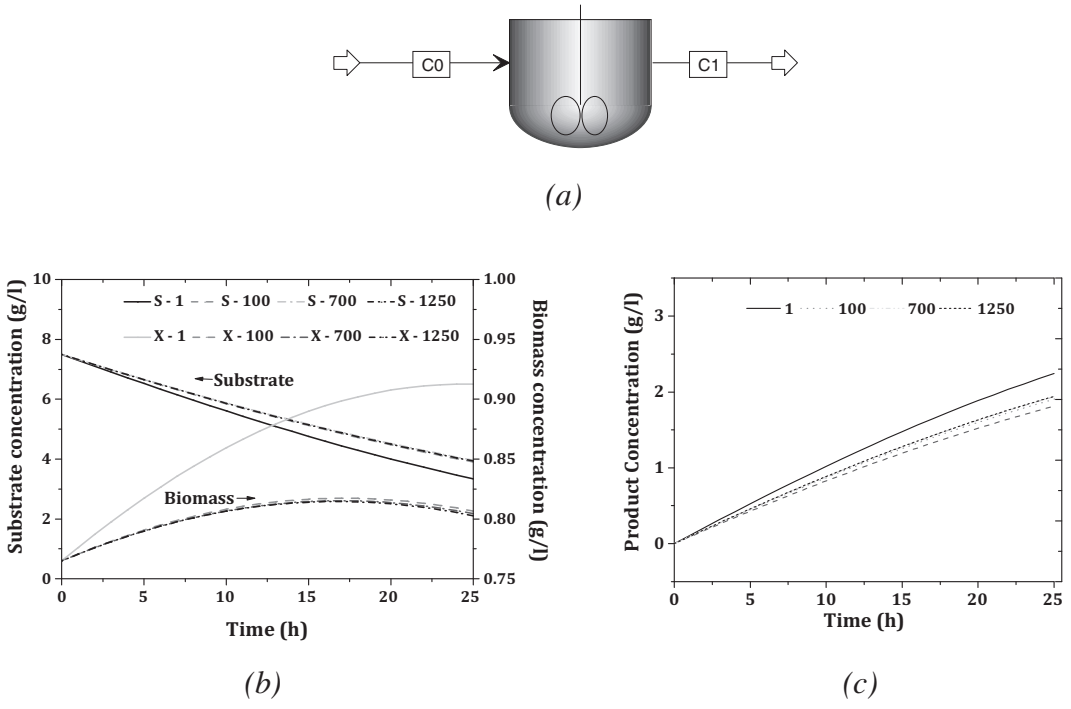

Fig. 1. Model (*i*). Scheme of the biomass-ethanol producing fermenter (a) and mean concentrations profiles as function of the number of scenarios (N = 1, 50, 100, 200, 700 and 1250) for substrate and biomass (b) and product (c).

Table 1
Uncertain parameters of the kinetic models.

Parameter	Description	Nominal value	Sd	Unit	Range	
					Min	Max
Model (i): Biomass and ethanol fermenter						
μ_{max}	Maximum specific growth rate of biomass	0.100[a]	0.015	h^{-1}	0.100[c,d]	1.000[e]
$Y_{x/s}$	Biomass yield coefficient	0.124[a]	0.020	–	0.001[d]	0.550[e]
$Y_{x/p}$	Product yield coefficient	0.230[a]	0.060	–	0.004[d]	0.600[f]
K_s	Substrate saturation constant	20.000[a]	2.500	kg/m^3	0.010[d]	20.000[a]
v_{dead}	Biomass death rate	0.020[a]	0.004	h^{-1}		
Model (ii): Bioreactor network						
$\mu_{max,1}$	Maximum specific growth rate of biomass	0.500[a]	0.060	h^{-1}	0.010[c,d]	1.000[e]
$\mu_{max,2}$	Maximum specific growth rate of biomass	0.100[a]	0.015	h^{-1}	0.100[d]	1.000[e]
$Y_{x/s,2}$	Biomass yield coefficient	0.124[a]	0.020	–	0.001[d]	0.550[e]
$Y_{x/p,2}$	Product yield coefficient	0.230[a]	0.060	–	0.004[d]	0.600[f]
K_s*	Substrate saturation constant	20.000[a]	2.500	kg/m^3	0.010[d]	20.000[a]
v_{dead}*	Biomass death rate	0.020[a]	0.004	h^{-1}		
Model (iii): Co-fermenter						
$\mu_{max,g}$	Maximum specific growth rate of biomass on glucose	0.662[b]	0.083	h^{-1}	0.010[c,d]	1.000[e]
$\mu_{max,x}$	Maximum specific growth rate of biomass on xylose	0.190 [b]	0.024	h^{-1}	0.017[d]	0.417[f]
$v_{max,g}$	Maximum specific rate of product formation from glucose	2.005 [b]	0.251	h^{-1}	2.005[b]	5.120[g]
$v_{max,x}$	Maximum specific rate of product formation from xylose	0.250 [b]	0.031	h^{-1}	0.250[b]	3.080[d]
$Y_{p/s,g}$	Yield coefficient for ethanol on glucose	0.470 [b]	0.059	–	0.294[a]	0.600[f]
$Y_{p/s,x}$	Yield coefficient for ethanol on xylose	0.400 [b]	0.05	–	0.350[h]	0.796[d]
λ	Glucose to total sugar concentration ratio in the feed	0.650 [b]	0.081	–		

* Are common parameters for both kinds of bioreactors in the network.
[a] Corsano et al. (2004).
[b] Krishnan et al. (1999).
[c] Todri et al.(2014).
[d] Moreno et al. (2013).
[e] Nielsen et al. (2003).
[f] Nakamura et al. (2001).
[g] Leksawasdi et al. (2001).
[h] Morales-Rodriguez et al. (2011b).

whereas distillery vinasses or distillery broth are the non-distilled residue in bioethanol production process. Model (*i*) consists of a bioethanol and biomass producing fermenter through dynamic mass balance equations for biomass, substrate, non-active biomass and product described by Eqs. (1)–(4).

Biomass

$$\frac{dX}{dt} = \mu X - v_{dead} X \tag{1}$$

Substrate

$$\frac{dS}{dt} = -\frac{\mu X}{Y_{x/s}} \tag{2}$$

Non-active biomass

$$\frac{dX_{dead}}{dt} = v_{dead} X \tag{3}$$

Product

$$\frac{dP}{dt} = \frac{\mu X}{Y_{x/p}} \tag{4}$$

Specific growth rate of biomass in the fermenter is Monod type kinetics described by

Growth rate

$$\mu = \mu_{max} \frac{S}{K_s + S} \tag{5}$$

In this model, there are 5 parameters: μ_{max}, maximum specific growth rate of biomass; $Y_{x/s}$, biomass yield coefficient, $Y_{x/p}$, product yield coefficient; K_s, substrate saturation constant and v_{dead}, biomass death rate, which are described in Table 1.

2.1.2. Model (ii)

This model represents a two-bioreactor network through Eqs. (6)–(19). The network consists of a series of two batch bioreactors fed with the same substrate as model (*i*). For this study, the optimal configuration, determined by Corsano et al. (2004), was adopted: one aerobic and one anaerobic reactor in series, as it is shown in Fig. 2(a). The first bioreactor (R_1) of the network is a pre-fermenter required to enhance the production of yeast biomass. Only biomass production takes place within this bioreactor, with mass balances described by Eqs. (6)–(8) for sub-index $i = 1$.

Biomass

$$\frac{dX_i}{dt} = \mu_i X_i - v_{dead} X_i \quad i = 1,2 \tag{6}$$

Substrate

$$\frac{dS_i}{dt} = -\frac{\mu_i X_i}{Y_{x/s_i}} \quad i = 1,2 \tag{7}$$

Non-active biomass

$$\frac{dX_{dead}}{dt} = v_{dead} X_i \quad i = 1,2 \tag{8}$$

Specific growth rate of biomass in the fermenter is also Monod type kinetics.

Growth rate

$$\mu_i = \mu_{max_i} \frac{S_i}{K_s + S_i} \quad i = 1,2 \tag{9}$$

In this case, the yield coefficient, $Y_{x/s,1}$, an empirical efficiency measure for the substrate-biomass conversion depending on the carbohydrate source is represented by Eq. (10) (Albernas-Carvajal et al., 2014). Variables x_{ij} represent the fraction of total reduced sugar provided by molasses ($j = 1$) and vinasses ($j = 2$) in bioreactor i

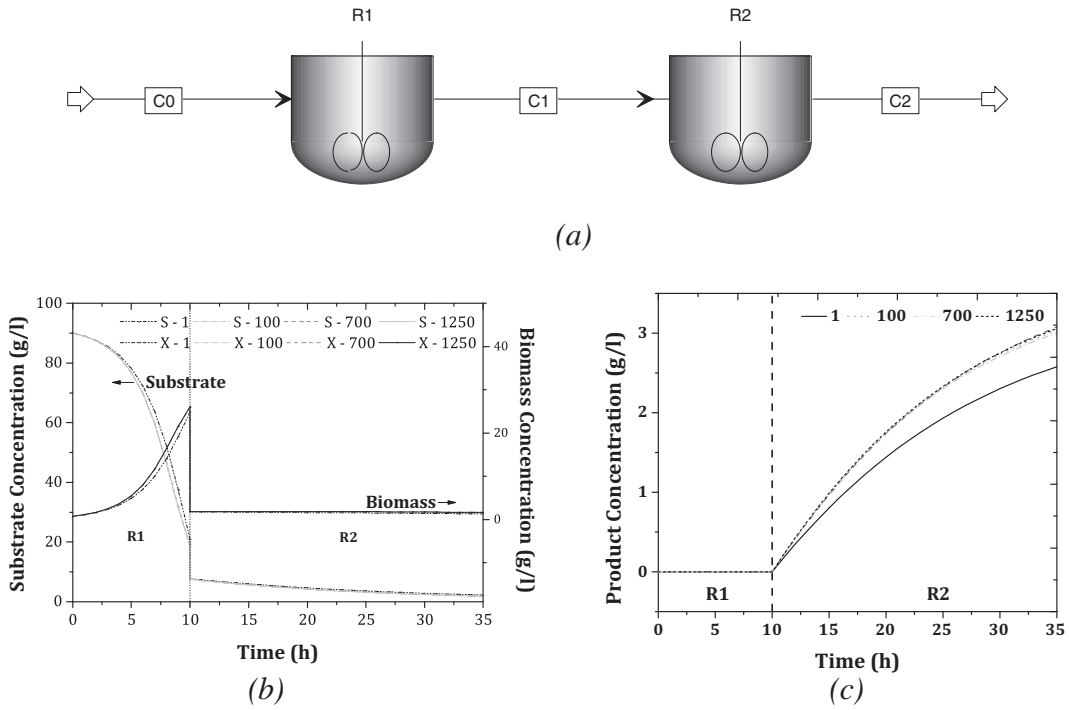

Fig. 2. Model (*ii*). Scheme of the bioreactor network (a) and mean concentration profiles as function of the number of scenarios ($N = 1$, 50, 100, 200, 700 and 1250) for substrate and biomass (b) and product (c).

Yield coefficient

$$Y_{xs,1} = 0.3689x_{1,1} + 0.2522x_{1,2} + 0.3736x_{1,1}x_{1,2} \tag{10}$$

$$x_{i,1} + x_{i,2} = 1 \quad i = 1,2 \tag{11}$$

The second bioreactor (R_2), where alcoholic fermentation occurs, is anaerobic to enhance bioethanol production. Dynamic mass balances are described by Eqs. (6)–(9) and Eq. (12) for sub-index $i = 2$.

Product

$$\frac{dP_i}{dt} = \frac{\mu_i X_i}{Y_{x/p_i}} \quad i = 2 \tag{12}$$

Eqs. (13)–(15) represent volume relations, where feed is composed of distillery vinasses and molasses volume. Inoculation only takes places in the first bioreactor.

Volume equations

$$FEED_i = DV_i + M_i \quad i = 1,2 \tag{13}$$

$$V_1 = FEED_1 + V_{inoc} \quad i = 1 \tag{14}$$

$$V_i = FEED_i + V_{i-1} \quad i > 1 \tag{15}$$

Each fermenter is fed with a blend of molasses and vinasses, their contribution fraction of TRSs is calculated by Eqs. (16)–(19) in order to obtain $Y_{x/s,1}$ value.

Feeding sugar contribution

$$V_i S_{i0} x_{1_i} = M_i S_M \quad i = 1 \tag{16}$$

$$V_i S_{i0} x_{1_i} = M_i S_M + V_{i-1} S_{i-1} x_{1_{i-1}} \quad i > 1 \tag{17}$$

$$V_i S_{i0} x_{2_i} = DV_i S_{DVi} \quad i = 1 \tag{18}$$

$$V_i S_{i0} x_{2_i} = DV_i S_{DV} + V_{i-1} S_{i-1} x_{2_{i-1}} \quad i > 1 \tag{19}$$

Note that for the biomass reactor, the substrate yield coefficient is calculated using expression (10), while for the bioethanol bioreactor the substrate and product yield coefficients $Y_{x/s,2}$ and $Y_{x/p,2}$ are constant and assumed as model parameters. The model has 6 parameters, which are shown in Table 1.

2.1.3. Model (iii)

Obtaining bioethanol from lignocellulosic materials is a current challenge for the biofuels industry in the world and has the potential for making a significant contribution to the solution of major renewable energy and environmental problems. Lignocellulosic feedstocks like wood, waste paper, agricultural residues and fast-growing energy crops have been identified as economical starting materials for bioethanol production. Lignocellulosic hydrolyzates contain both fermentable sugars: pentoses and hexoses. Pentoses are comprised of D-xylose and L-arabinose whereas the major hexose is D-glucose. Advances in genetic engineering have led to the construction of xylose-fermenting microorganisms. The use of *Saccharomyces* yeast is highly favored in commercial biomass to bioethanol conversion processes owing to their traditional use, their tolerance to bioethanol and other inhibitors, GRAS (Generally Regarded As Safe) status, and their use as nutrient enhancers in animal feed. Ho et al. (1998) reported the development of effective recombinant yeast such as *Saccharomyces* 1400 (pLNH33), capable of simultaneously co-ferment glucose and xylose in the same medium to bioethanol with high bioethanol yields. However, both sugars metabolism and bioethanol production can be inhibited by toxic compounds generated during the acid hydrolysis of lignocellulose (Moreno et al., 2013). For the sake of simplicity, this kind of inhibition was not considered in the kinetic model. In this paper a kinetic co-fermentation model proposed by Krishnan et al. (1999) to describe cell growth and product formation of *Saccharomyces* 1400(pLNH33) on glucose and xylose mixtures was implemented. Eqs. (20)–(23) represent the dynamic mass balances for product obtained either from glucose or xylose, glucose and xylose, respectively. The model incorporates the effect of substrate inhibition on cell growth and bioethanol production using glucose and xylose as substrate through a modified Monod form expression. In addition, a two constant model is used to describe the kinetic pattern of bioethanol inhibition on glucose and xylose fermentation.

Product from glucose

$$\frac{dP_g}{dt} = \frac{v_{max_g} s_g}{K'_g + s_g + (s_g^2/K'_{i,g})} \left\{ 1 - \left(\frac{p_g}{p'_{max_g}} \right)^{\varphi_g} \right\} X \tag{20}$$

Product from xylose

$$\frac{dP_x}{dt} = \frac{v_{max_x} s_x}{K'_x + s_x + (s_x^2/K'_{i,x})} \left\{ 1 - \left(\frac{p_x}{p'_{max_x}} \right)^{\varphi_x} \right\} X \tag{21}$$

Glucose

$$\frac{dS_g}{dt} = -\frac{1}{Y_{p/s_g}} \frac{v_{max_g} s_g}{K'_g + s_g + \left(s_g^2/K'_{i,g}\right)} \left\{ 1 - \left(\frac{p_g}{p'_{max_g}} \right)^{\varphi_g} \right\} X \tag{22}$$

Xylose

$$\frac{dS_x}{dt} = -\frac{1}{Y_{p/s_x}} \frac{v_{max_x} s_x}{K'_x + s_x + (s_x^2/K'_{i,x})} \left\{ 1 - \left(\frac{p_x}{p'_{max_x}} \right)^{\varphi_x} \right\} X \tag{23}$$

Model of biomass growth on sugar mixtures, represented by Eq. (24), considers that competition for uptake occurs between the two substrates.

Biomass

$$\frac{dX}{dt} = \left[\frac{s_g}{s_g + s_x} \frac{\mu_{max_g} s_g}{K_g + s_g + (s_g^2/K_{i,g})} \left\{ 1 - \left(\frac{p_g}{p_{max_g}} \right)^{\phi_g} \right\} + \frac{s_x}{s_g + s_x} \frac{\mu_{max_x} s_x}{K_x + s_x + (s_x^2/K_{i,x})} \left\{ 1 - \left(\frac{p_x}{p_{max_x}} \right)^{\phi_x} \right\} \right] X \tag{24}$$

Eqs. (25) and (26) represent both glucose and xylose conversion with respect to fed sugar concentration (Chen and Wang, 2010).

Glucose conversion

$$\chi_g = 1 - \frac{s_g}{\lambda s_f} \tag{25}$$

Xylose conversion

$$\chi_x = 1 - \frac{s_g}{(1-\lambda) s_f} \tag{26}$$

There are 23 parameter in this model described in the nomenclature section together with their nominal value. The model parameters in the substrate and product inhibition expressions were determined from single substrate experiments by Krishnan et al. (1999). Table 1 includes description, nominal value, standard deviation considered for the GSA and range of variation taken from literature of uncertain parameters.

2.2. Global sensitivity analysis

Sensitivity analysis can be defined as the study of how uncertainty in model dependent variables can be assigned to different sources of uncertainty in model parameters (Saltelli et al., 2008). Sensitivity analysis can be addressed through local and global methodologies.

Local techniques evaluate sensitivity indices as first order partial derivatives of dependent variables with respect to uncertain parameters, based on Taylor's series expansion around the parameters nominal value. However, the assumption of linearity is usually valid only within a narrow range of parameter variation. Thus, results obtained from local sensitivity analysis cannot be representative when nonlinear models and the entire space of parameter variation are considered.

On the other hand, global sensitivity analysis is based on the exploration of the entire range of parameter variation, sampling from a distribution function associated to each input parameter and simulating the model repeatedly. Even when the computational cost for global sensitivity methods is higher than for local sensitivity approaches, the former provide more reliable and realistic results, also taking into account the interaction between parameters (Saltelli et al., 2008).

In this work Sobol's method is used to compute sensitivity indices. This method is based on variance decomposition, using Monte-Carlo simulation methods (Sobol', 2001; Saltelli and Tarantola, 2002).

Given a function $y = f(x, t)$, where y is a differential or algebraic state variable (such as biomass concentration), $\boldsymbol{x}$ is a vector of k input parameters and t is the independent variable in differential equations, e.g., time; when all uncertain parameters x_i vary under its probability density function, the uncertainty of $y(x, t)$ can be quantify by its unconditional variance $V(y)$. To determine the contribution of each parameter on the unconditional variance the concept of conditional variance is introduced. Based on probability theory, the unconditional variance can be decomposed as the sum of the variance of a conditional expected value and the expected value of a conditional variance:

$$V(y) = V(E(y|x_i)) + E(V(y|x_i)) \tag{27}$$

$$V(y) = V(E(y|x_{-i})) + E(V(y|x_{-i})) \tag{28}$$

V and E correspond to variance and expected value operators, respectively. In Eq. (27), $V_i = V(E(y|x_i))$ computes the variance (over all possible realizations of parameter x_i) of the conditional expected value of the state variable y under all parameters variation, except x_i. It represents the expected reduction in the state variable variance that could be obtained if x_i could be known or fixed. V_i is the first-order effect associated to parameter x_i. The second term, $E_i = E(V(y|x_i))$, is the expected value (over all realizations of parameter x_i.) of the conditional variance of the state variable y when all parameters except x_i change. It represents the average state variable variance if x_i could be known or fixed.

The same can be stated for Eq. (28), by replacing x_i for "all parameters except x_i" (x_{-i}). Thus, the term $V_i^{TOT} = E(V(y|x_{-i}))$ computes the average state variable variance if all parameters except x_i could be known or fixed.

If Eqs. (27) and (28) are divided by the unconditional variance, the following expressions are obtained:

Table 2
Steps for computing sensitivity indices.

Step	Calculations
1.	Generate two random sets of model parameters, $\alpha = (\eta, \zeta)$ and $\beta = (\eta', \zeta')$ matrices – Matrices dimension: $N \times k$ – η, vector $(N \times 1)$ of random values for parameter x_i – ζ, submatrix $(N \times (k-1))$ of random values for all parameter except x_i
2.	Define a new matrix $\gamma_i = (\eta, \zeta')$ – Matrix γ_i formed by all columns of β except the ith column, which is taken from α
3.	Calculation of state variables for all parameter values in the sample matrices of Steps 1 and 2 – Three vectors $(N \times 1)$ of state variables are obtained, $y_\alpha = f(\alpha)$, $y_\beta = f(\beta)$, $y_{\gamma i} = f(\gamma_i)$
4.	Calculation of variance and conditional variances for state variables, at each time instant. – Defined by Eqs. (43)–(45)
5.	Calculation of sensitivity indices at each time instant

Table 3
Influence of parameters based on its indices values.

Indices	Relative value	Condition for parameter x_i
S_i	High	Influential parameter
S_i^{int}	High	Important interactions between x_i and other parameters
S_i^{int}	Small	Little or no interactions between x_i and other parameters
S_i and S_i^{TOT}	Small	Non influential parameter

S_i, S_i^{int} and S_i^{TOT} stand for first order, interactional and total sensitivity index for parameter *i*.

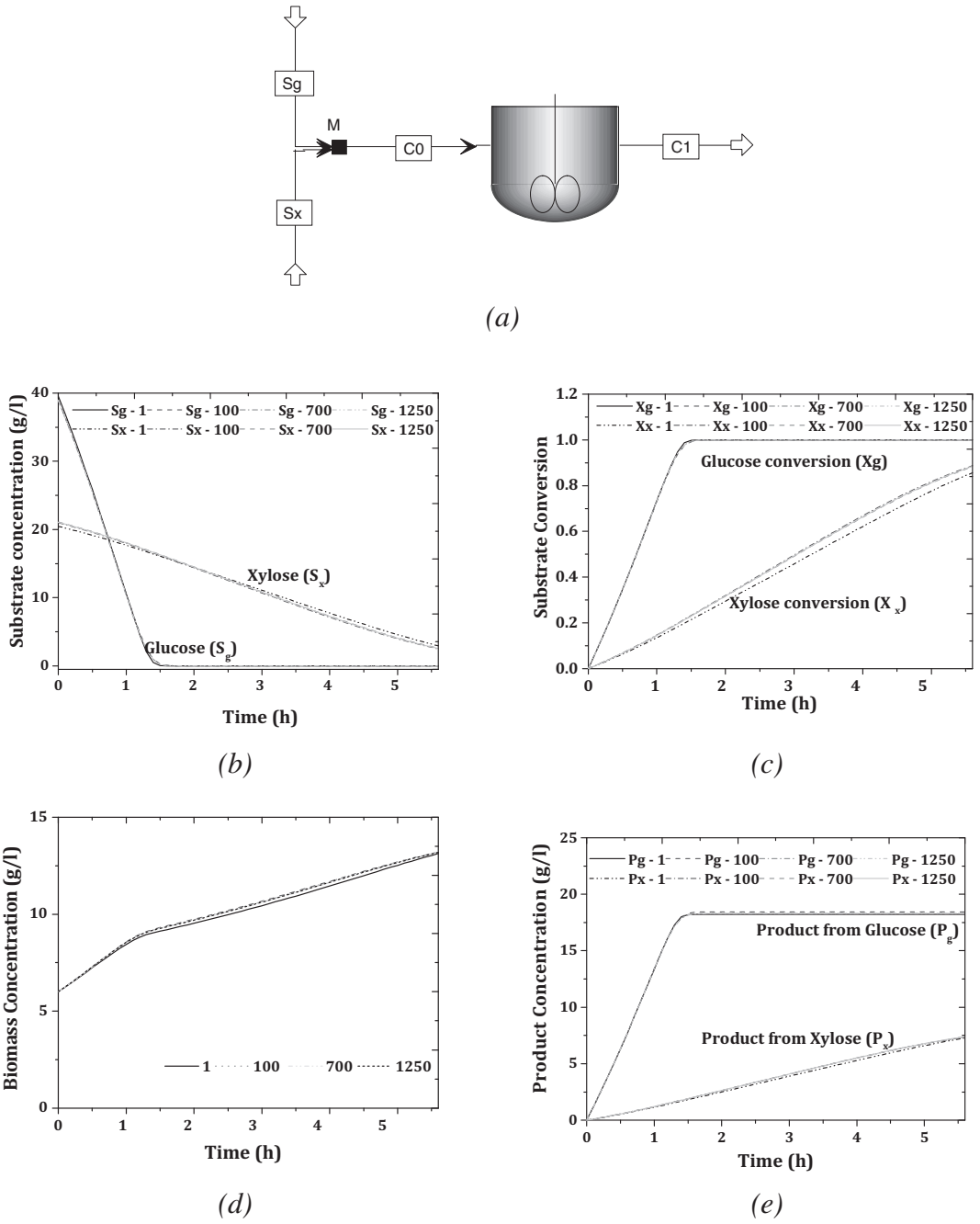

Fig. 3. Model (*iii*). Scheme of ethanol co-fermentation bioreactor (a) and mean concentration profiles as function of the number of scenarios (N = 1, 50, 100, 200, 700 and 1250) for glucose (S_g) and xylose (S_x) (b), glucose (χ_g) and xylose (χ_x) conversion (c), biomass (d) and product from glucose (P_g) and from xylose (P_x) (e).

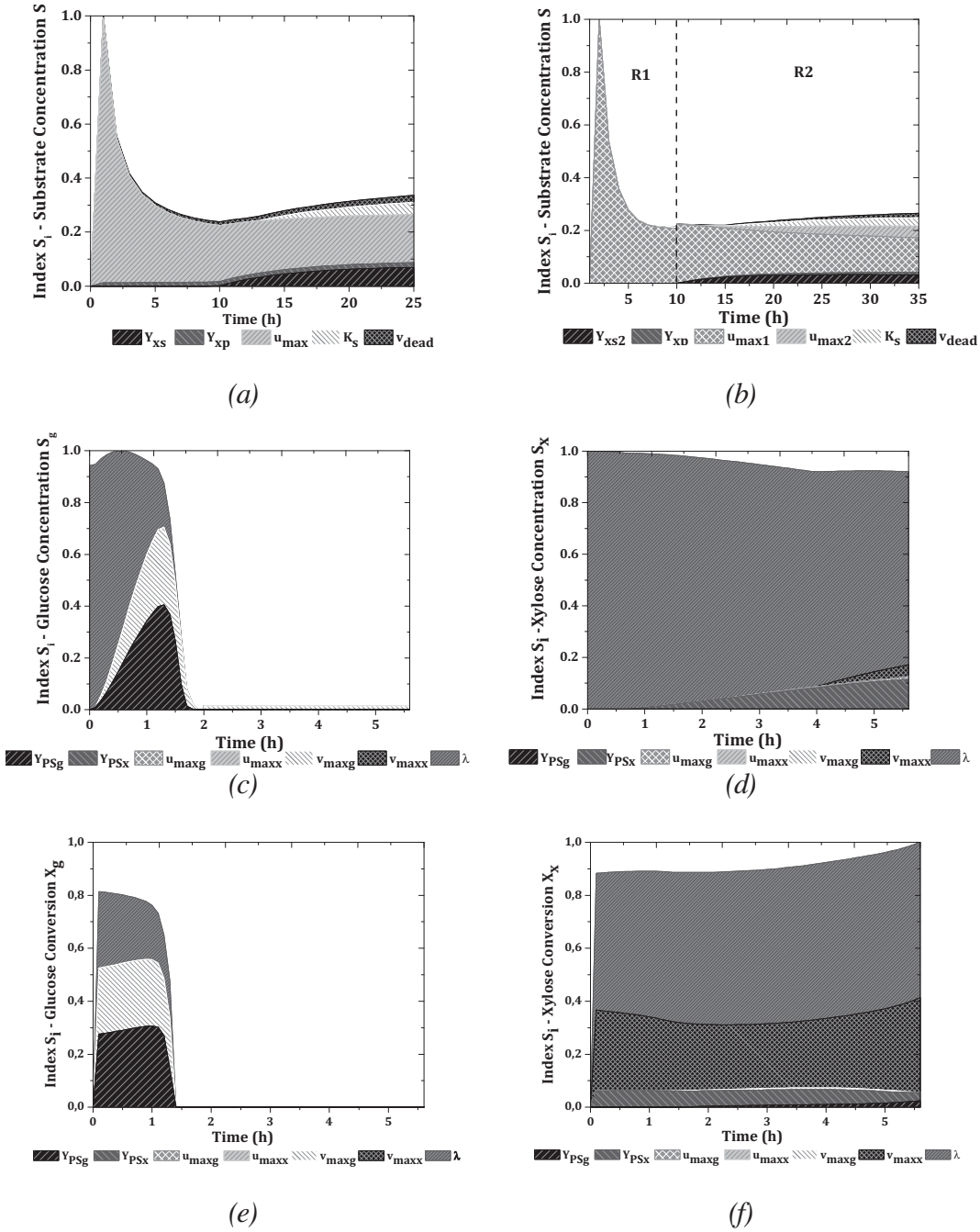

Fig. 4. First order sensitivity index profiles for substrate concentration and substrate conversion. Substrate concentration for biomass-ethanol producing fermenter (model (*i*)) (a), substrate concentration for bioreactor network (model (*ii*)) (b) and glucose (c) and xylose (d) concentrations and glucose (e) and xylose (f) conversions profiles for co-fermentation bioreactor (model (*iii*)).

$$1 = \frac{V(E(y|x_i))}{V(y)} + \frac{E(V(y|x_i))}{V(y)} \tag{29}$$

$$1 = \frac{V(E(y|x_{-i}))}{V(y)} + \frac{E(V(y|x_{-i}))}{V(y)} \tag{30}$$

Finally, the first-order sensitivity index, S_i and the total sensitivity index S_i^{TOT} are defined as:

$$S_i = \frac{V(E(y|x_i))}{V(y)} = \frac{V_i}{V(y)} \tag{31}$$

$$S_i^{TOT} = \frac{E(V(y|x_{-i}))}{V(y)} = \frac{V_i^{TOT}}{V(y)} \tag{32}$$

As it can be seen from Eqs. (31) and (32), to calculate sensitivity indices is necessary to compute the unconditional and conditional variances of each state variable and these involve the calculation of multiple integrals. Sobol' proposes a methodology to compute the variances considering only evaluations of functions ($y = f(x, t)$), a brief description of this methodology is given below. A square integrable function $y = f(x, t)$ was considered, where y is a differential or algebraic state variable (such as biomass concentration), $\boldsymbol{x}$ is a vector of k input parameters and t is the independent variable in differential equations, e.g., time. For the sake of clarity, subscript t is omitted in the following analysis, assuming f, its expected value and its variance are calculated at each time instant. Function f can be decomposed into terms of increasing dimensions (Sobol', 2001), as follows:

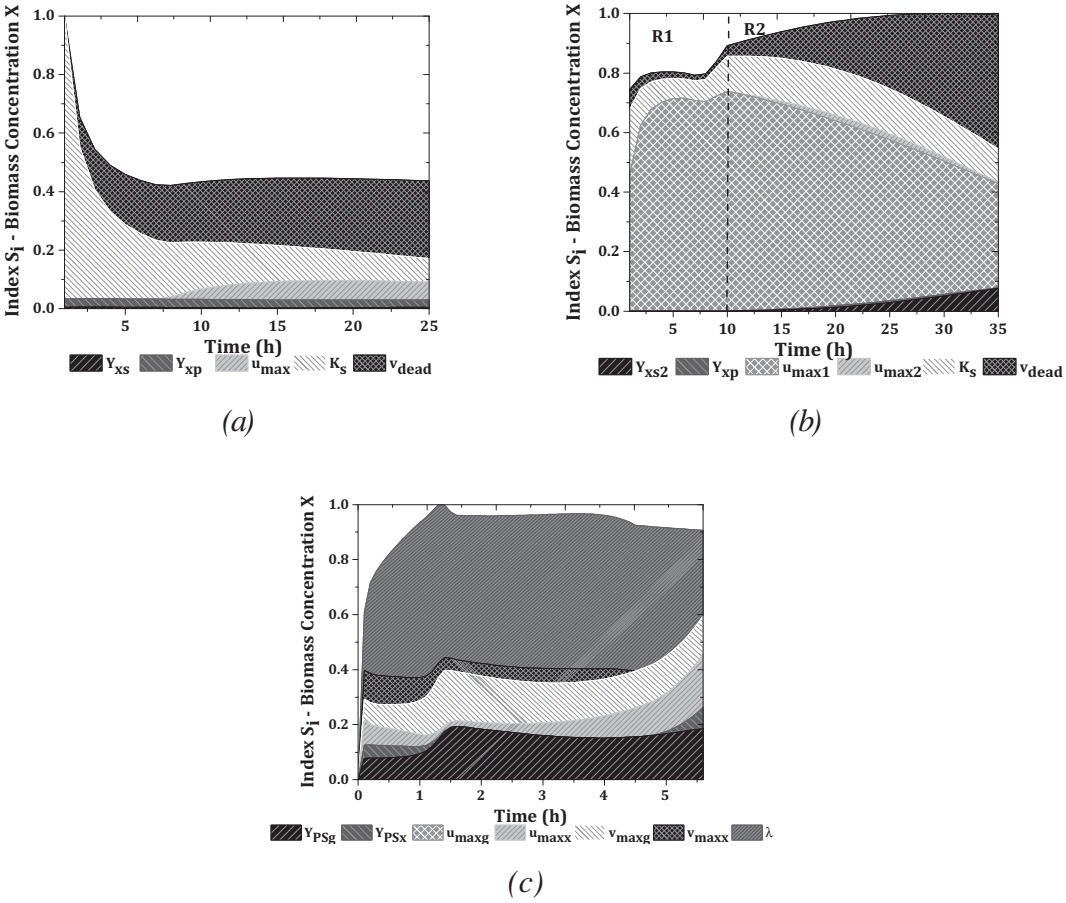

Fig. 5. First order sensitivity index profiles for biomass concentration. Biomass-ethanol producing fermenter (model (*i*)) (a), bioreactor network (model (*ii*)) (b) and co-fermentation bioreactor (model (*iii*)) (c).

$$f = f_0 + \sum_i f_i(x_i) + \sum_i \sum_{j>i} f_{ij}(x_i, x_j) + \cdots + f_{12\ldots k}(x_i, x_j, \ldots, x_k) \quad (33)$$

where each term is also square integrable and is a function of the factors in its index, i.e., $f_i = f_i(x_i)$, $f_{ij} = f_{ij}(x_i, x_j)$ and so on.

This expansion is called High Dimensional Model Representation (HDMR). Sobol' proved that if each term of the expansion has zero mean, i.e.:

$$\int_0^1 f_{i_1\ldots i_s}(x_{i_1}\ldots x_{i_s})dx_n = 0 \quad (34)$$

then all the terms of the decomposition are orthogonal in pairs:

$$\int_0^1 \int_0^1 f_{i_1\ldots i_s} f_{k_1\ldots k_l} dx_i dx_k = 0 \quad (35)$$

As a consequence, all terms in Eq. (33) can be univocally calculated using the conditional expectations of the state variable y, as

$$E(y) = \int f(x)dx = f_0 \quad (36)$$

$$E(y|x_i) = \int f(x)\prod_{k\neq i} dx_k = f_0 + f_i(x_i) \quad (37)$$

Eq. (36) corresponds to the definition of the expected value of a variable y which is function of uncertain variables. Eq. (37) is the definition of conditional expected value of a variable **y** when x_i is known, and it is obtained integrating Eq. (33) over all variables except x_i.

By square integrating each term of Eq. (33)

$$\int\int\cdots\int f^2(x)dx_i\ldots dx_n - f_0^2 = \sum_{s=1}^{k}\sum_{i_1<\ldots<i_s}^{k}\int\int\cdots\int f_{i_1\ldots i_s}^2 dx_{i_1}\ldots dx_{i_s} \quad (38)$$

where

$$V(y) = \int\int\cdots\int f^2(x)dx_i\ldots dx_n - f_0^2 \quad (39)$$

$$V_{i_1\ldots i_s} = \int\int\cdots\int f_{i_1\ldots i_s}^2 dx_{i_1}\ldots dx_{i_s} \quad (40)$$

$V(y)$ and $V_{i_1\ldots i_s}$ are the unconditional and conditional variance of the state variable respectively. Then, the so-called ANOVA-HDMR decomposition can be derived,

$$V(y) = \sum_i V_i + \sum_i \sum_{j>i} V_{ij} + \ldots + V_{12\ldots k} \quad (41)$$

Dividing both sides of the equation by $V(y)$ the index decomposition is obtained:

$$1 = \sum_i S_i + \sum_i \sum_{j>i} S_{ij} + \sum_i \sum_{j>i} \sum_{l>j} S_{ijl} \cdots + S_{123\ldots k} \quad (42)$$

In this work, the methodology was implemented following Saltelli and Tarantola (2002) which is an extension of the original approach proposed by Sobol' (1993) and Homma and Saltelli (1996). This procedure computes the variances based on model evaluations, as defined by Eqs. (43)–(45).

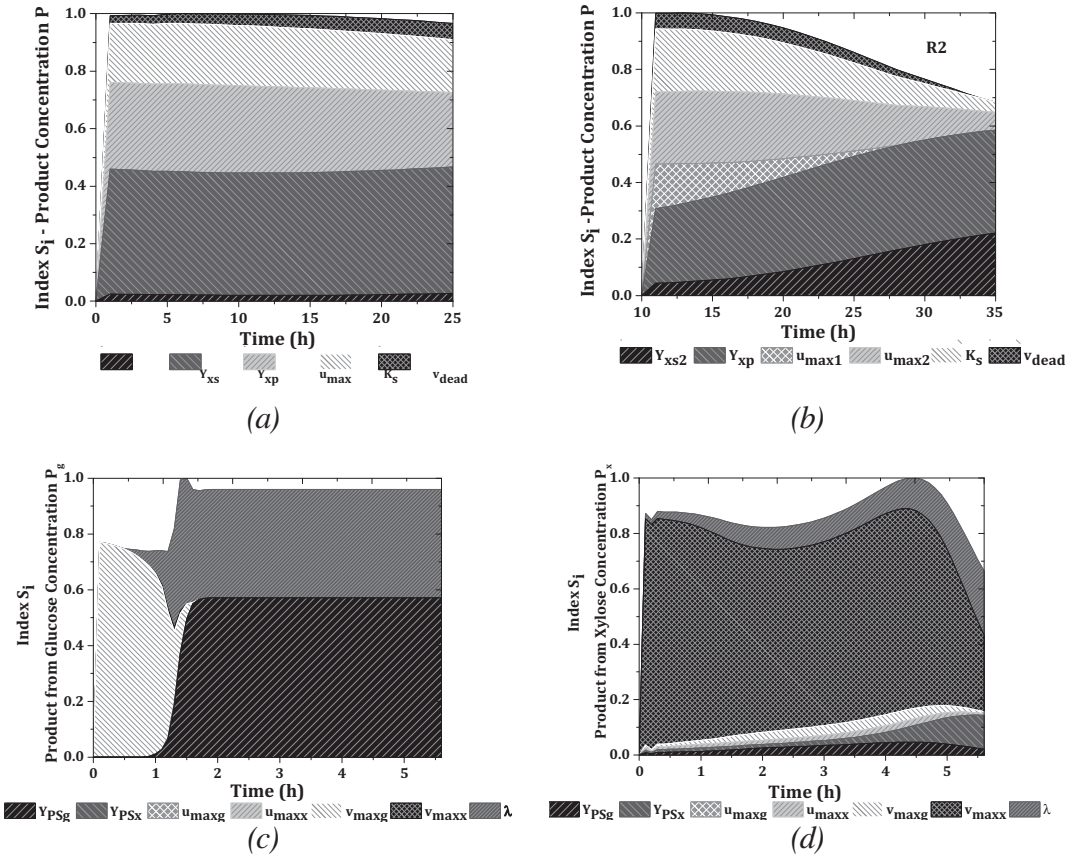

Fig. 6. First order sensitivity index profiles for product concentration. Biomass-ethanol producing fermenter (model (*i*)) (a), bioreactor network (model (*ii*)) (b) and concentration product from glucose (c) and xylose (d) for the co-fermentation bioreactor (model (*iii*)).

$$V(y) = \frac{1}{N}\left(\sum_{j=1}^{N}(y_{\alpha}^{j})^2 - \sum_{j=1}^{N} y_{\alpha}^{j} y_{\beta}^{j}\right) \tag{43}$$

$$V(E(y|x_i)) = \frac{1}{N}\left(\sum_{j=1}^{N} y_{\alpha}^{j} y_{\gamma_i}^{j} - \sum_{j=1}^{N} y_{\alpha}^{j} y_{\beta}^{j}\right) i = \quad 1 \ldots k \tag{44}$$

$$V(E(y|x_{-i})) = \frac{1}{N}\left(\sum_{j=1}^{N} y_{\beta}^{j} y_{\gamma_i}^{j} - \sum_{j=1}^{N} y_{\alpha}^{j} y_{\beta}^{j}\right) \quad i = 1 \ldots k \tag{45}$$

where N is the number of scenarios for the Monte Carlo simulations; α, β and γ_i are matrices of N random values for the k uncertain model parameters and y_{α}, y_{β} and $y_{\gamma i}$ are vectors of N model outputs values obtained when model variables are evaluated in matrices α, β and γ_i, respectively. The main steps for the case of a differential algebraic model are described in Table 2.

First order (S_i) and total effect (S_i^{TOT}) indices measure the effect of the variation of the parameters on the model state variables. First sensitivity indices provide the reduction on the unconditional variance of the state variable that can be obtained if x_i is fixed at its true value. On the other hand, total sensitivity indices take into account the interactions among parameters, so they give information on the non-additive part of the model.

Usually, $\sum_{i=1}^{k} S_i < 1$ and $S_i < S_i^{TOT}$. However for a purely additive model and orthogonal inputs, $\sum_{i=1}^{k} S_i = 1$, which can be observed from Eq. (42) when the interaction terms are canceled.

An additional index, S_i^{int} takes into account the effects of all interactions among model parameters and it can be calculated as:

$$S_i^{int} = S_i^{TOT} - S_i \tag{46}$$

Table 3 gives information on the influence of parameter x_i based on the value of its indices.

3. Results and discussion

A dynamic global sensitivity analysis was carried out on the previously described bioreactor models comprising differential algebraic systems of equations. The DAE models were implemented in an equation-oriented environment, within gPROMS (PSEnterprise Ltd., 2014).

The model (*i*) has 4 differential and 1 algebraic equations and 5 parameters; in model (*ii*), there are 7 differential and 14 algebraic equations and 6 parameters and in model (*iii*), there are 5 differential and 2 algebraic equations and 23 parameters. For models (*i*) and (*ii*), GSA was carried out over all model parameters (5 and 6, respectively), which are shown in Table 1. To reduce the number of uncertain parameters in model (*iii*) over which GSA was applied, and hence the computational effort, a preliminary screening through local sensitivity analysis was carried out on the entire set of model parameters. By taking into account only those parameters that have a greater impact in the model output, the following parameters for GSA were selected: $\mu_{max,g}$, $\mu_{max,x}$, $v_{max,g}$, $v_{max,x}$, $Y_{p/s,g}$, $Y_{p/s,x}$ and λ. Normal probability distributions were associated to uncertain parameters. Mean values and standard deviations were estimated based on information from the literature. Parameter nominal values were considered as their mean values and 12.5% standard deviations. In general, this represents a typical range of variation of parameters. Matrices of random parameters α, β and γ_i were generated for each DAE model within gPROMS to perform stochastic simulations.

Table 4
Substrate concentration sensitivity indices.

Model (*i*)						Model (*ii*)						Model (*iii*)											
S						*S*						S_g						S_x					
S_i			S_i^{int}			S_i			S_i^{int}			S_i			S_i^{int}			S_i			S_i^{int}		
$t = 2$	$t = 5$	$t = 25$	$t = 2$	$t = 5$	$t = 25$	$t = 2$	$t = 5$	$t = 25$	$t = 2$	$t = 5$	$t = 25$	$t = 1$	$t = 2$	$t = 5$	$t = 1$	$t = 2$	$t = 5$	$t = 1$	$t = 2$	$t = 5$	$t = 1$	$t = 2$	$t = 5$
$Y_{x/s}$		0.07	**1.14**	**0.72**	**0.33**	$Y_{x/s,2}$		0.03	**0.76**		0.06	$Y_{p/s,g}$	**0.34**										
$Y_{x/p}$	0.01	0.02				$Y_{x/p,2}$		0.01	**0.76**		0.03	$Y_{p/s,x}$			0.06	0.04	0.04	0.01	0.03	0.1			
μ_{max}	**0.54**	**0.18**			0.05	$\mu_{max,1}$	**1**	**0.15**		**0.2**	**0.51**	$\mu_{max,g}$			0.05	**0.36**	**0.36**			0.01			
K_s	0.05				0.11	$\mu_{max,2}$		0.03	**0.76**	**0.3**	0.10	$\mu_{max,x}$			0.06								
v_{dead}	0.01	0.03				K_s		0.02	**3.14**	**0.3**	**0.20**	$v_{max,g}$	**0.26**	0.01	0.01	0.06	**0.87**	**0.87**			0.03	0.05	0.06	0.06
						v_{dead}		0.01	**1.06**	0.01	0.03	$v_{max,x}$				0.06	0.02	0.02						
												λ	**0.36**			0.14			**0.98**	**0.94**	**0.78**			
Σ	0.56	0.31	0.34				1.00	0.28	0.25			Σ	0.96	0.01	0.01				0.99	0.97	0.92			

Sub-index 1, 2, *g* and *x* stands for biomass production bioreactor, ethanol production bioreactor, glucose and xylose respectively. S_i and S_i^{int} represent first order and interactional sensitivity indices for parameter *i*. *t*: time (h). The highest values obtained are marked in bold.

The number of scenarios for each model has been estimated by performing stochastic simulations for increasing number of scenarios (N = 1, 100, 700 and 1250) (Estrada and Diaz, 2010) and comparing mean concentration profiles for substrate, biomass, product and substrate conversion. As it can be seen in Fig. 1 (b) and (c) for model (*i*), Fig. 2(b) and (c) for model (*ii*) and Fig. 3 (b)–(e) for model (*iii*), the main differential state variables (substrate, biomass and product concentrations) and algebraic state variables (substrate conversions profiles) mean profiles remain unchanged for N = 1250 scenarios. So, 1250 scenarios were considered as representative for the whole set of possible scenarios.

Stochastic simulations, conditional and unconditional variances and sensitivity index calculations for the different set of parameters for each time instant have been carried out in gPROMS (PSEnterprise Ltd., 2014).

GSA results for three differential state variables (substrate, biomass and product concentration) and two algebraic state variables (glucose and xylose conversion) are presented in cumulative plots and tables for the three studied models. Figs. 4–6 show temporal profiles for first order sensitivity (S_i) while Tables 4–6 show first order (S_i) and interactions (S_i^{int}) indices at three reactions times. In the following discussion, each state variable global sensitivity analysis was addressed with respect to parameters for each analyzed model.

3.1. Substrate concentration

In the biomass-ethanol producing fermenter, model (*i*), substrate concentration *S* (Fig. 4(a) and Table 4) is mainly influenced throughout the entire horizon of time by μ_{max}, which represents the maximum specific growth rate of biomass, explaining between 20% and 100% of substrate concentration variance with first order effects, with the maximum contribution at the beginning of the fermentation. The biomass yield coefficient $Y_{x/s}$ explains up to 7% of the variance at the end of the time horizon, with the most important contribution through its interactions with other parameters (S^{int} between 0.33 and 1.14) (Table 4).

In model (*ii*), the biomass-ethanol bioreactor network, the most influential parameter for substrate concentration (*S*) is $\mu_{max,1}$, the maximum specific growth rate in the first reactor, which explains between 25% and 100% of substrate concentration variance in the network, being higher at the beginning of the process (Fig. 4(b)). As it can be seen in Table 4, $\mu_{max,1}$ also contributes to uncertainty in substrate concentration through its interactions with other parameters (S^{int} up to 0.51 at the end of the time horizon). In model (*ii*), at the beginning of the fermentation process (after t = 10 h), the following parameters are influential, to a lesser extent: $Y_{x/s,2}$ (biomass yield coefficient), $\mu_{max,2}$ (maximum specific growth rate for the second reactor) and K_s (substrate saturation constant). These results are consistent with the fact that growth is the main process in the first bioreactor (R_1), but biomass concentration (dependent on substrate concentration) also influences the rest of the process. Fig. 4(b) and Table 4 show that in model (*ii*), $Y_{x/s,2}$ is the second most influential parameter in first order effect after 10 h and, at the same time, it is the main parameter involved in interactions (S^{int}) along the entire time horizon. However, this kind of effect at the first stage of the network (R_1) can be attributed to K_s and v_{dead}, which represent substrate saturation constant and biomass death rate respectively; and then to $\mu_{max,1}$ and K_s. The presence of interaction effects reveals that the model is non-additive.

In model (*iii*), which corresponds to a bioreactor where co-fermentation of glucose and xylose takes place, there is a well-known preference of the engineered yeast for the first substrate. Glucose (S_g) is totally consumed at time t = 1.5 h, when only 20% xylose (S_x) has been consumed, as it can be seen in conversion profiles mean values shown in Fig. 3(c).

Table 5
Biomass concentration sensitivity indices.

	Model (*i*)							Model (*ii*)							Model (*iii*)						
	X							*X*							*X*						
	S_i			S_i^{int}				S_i			S_i^{int}				S_i			S_i^{int}			
	t = 2	*t* = 5	*t* = 25	*t* = 2	*t* = 5	*t* = 25		*t* = 2	*t* = 5	*t* = 25	*t* = 2	*t* = 5	*t* = 25		*t* = 1	*t* = 2	*t* = 5	*t* = 1	*t* = 2	*t* = 5	
$Y_{x/s}$	0.01	0.01	0.01				$Y_{x/s,2}$			0.03		0.02	0.05	$Y_{p/s,g}$	0.09	**0.2**	**0.2**				
$Y_{x/p}$	0.03	0.03	0.02				$Y_{x/p,2}$			0.01		0.02	0.09	$Y_{p/s,x}$	0.03		0.01				
μ_{max}			0.06	**0.65**	**0.42**	0.06	$\mu_{max,1}$	0.63	0.71	**0.54**	**0.54**	**0.4**	**0.38**	$\mu_{max,g}$				0.14	0.13	**0.15**	
K_s	**0.52**	**0.25**	0.08				$\mu_{max,2}$			0.02		0.02	0.1	$\mu_{max,x}$	0.04	0.02	0.14				
υ_{dead}	0.10	**0.17**	**0.27**			0.11	K_s	0.12	0.07	**0.15**				$\nu_{max,g}$	0.12	0.2	0.14				
							υ_{dead}	0.04	0.02	**0.25**				$\nu_{max,x}$	0.08	0.05					
														λ	**0.56**	**0.5**	**0.5**				
Σ	0.65	0.46	0.44					0.79	0.80	1.00				Σ	0.92	0.96	0.93				

Sub-index 1, 2, *g* and *x* stands for biomass production bioreactor, ethanol production bioreactor, glucose and xylose respectively. S_i and S_i^{int} represent first order and interactional sensitivity indices for parameter *i*. *t*: time (h). The highest values obtained are marked in bold.

Fig. 4(c) shows that until *t* = 1.5 h, λ (glucose-to-total sugar concentration ratio in the feed), $Y_{p/s,g}$ (yield coefficient for ethanol) and $\nu_{max,g}$ (maximum specific rate of product formation) are the most influential parameters, explaining 100% of glucose concentration variance. After *t* = 1.5 h (when glucose is depleted), only the effect of interaction between parameters are important (Table 4) again being $Y_{p/s,g}$ and $\nu_{max,g}$ the most important together with $\mu_{max,g}$ (maximum specific growth rate of biomass on glucose). For xylose concentration (Fig. 4(d)), the most influential parameter throughout the entire time horizon is λ, which explains almost 100% of the total variance. The effects of interactions among uncertain parameters (S_i^{int}) are negligible, as compared to first order effects (S_i), as it can be seen in Table 4. Consequently, total variance for xylose concentration can be explained only by first order effects of λ.

3.2. Conversion

In this section, temporal profiles for sensitivity indices corresponding to two algebraic state variables of model (*iii*): glucose (Fig. 4(e)) and xylose (Fig. 4(f)) conversion (x_x and x_g, respectively) were analyzed. Fig. 4(e) shows cumulative plots of first order indices for glucose conversion. There are only three relevant parameters, $Y_{p/s,g}$, λ, and $\nu_{max,g}$ that account for 80% of glucose conversion variance for time $t < 1.5$ h; this effect vanishes along the time horizon, together with glucose depletion. Interaction effects are totally negligible for this variable.

Fig. 4(f) show first order sensitivity indices profile for xylose conversion. First order effects explain more than 80% of this variable total variance and are dominated by λ with an almost constant value of S_i of 60%, followed by $\nu_{max,x}$ which contributes around 30% to xylose conversion variance. Finally, $Y_{p/s,x}$ explains around 6% of the uncertainty in xylose conversion along the time horizon.

3.3. Biomass concentration

First order sensitivity indices profiles for biomass concentration (*X*) are shown in Fig. 5(a)–(c), whereas interaction indices results are shown in Table 5. In model (*i*), first order effects of parameters explain 50% of biomass concentration variance, mainly contributed by K_s and ν_{dead}, being K_s, the substrate saturation constant, dominant at the beginning of the fermentation (almost 100%) and ν_{dead} contributing between 10 and 27% at the beginning and the end of the fermentation process, respectively (Fig. 5(a) – Table 5). Parameter μ_{max}, maximum specific growth rate of biomass in this fermenter, contributes with 6% of first order effects but it is the most important regarding its contribution by interaction with other parameters (S^{int}), which explains between 65% and 6% along the fermentation process (Table 5). Biomass and product yield coefficients only contribute together with 4% of biomass concentration variance as first order effects and do not contribute in interactions with other parameters. Therefore, these two parameters can be regarded as the less influential parameters in biomass concentration of model (*i*).

First order effects explain between 79% and 100% variance of yeast biomass concentration (*X*) in the biomass-fermenter network, model (*ii*) Fig. 5(b) and Table 5. It is mainly influenced by $\mu_{max,1}$, maximum specific growth rate of biomass, contributing between 54% and 71% (Table 5). It is followed by ν_{dead} which becomes important at the later stages of the process (25%), when fermentation metabolism dominates (Fig. 5(b)). K_s is also an important parameter, as it explains between 12% and 15% of biomass variance along the time horizon. Regarding interactions with other parameters, $\mu_{max,1}$ provides also the most significant contribution, between 35% and 54%. It is concluded that $\mu_{max,1}$ is the most influential parameter in the biomass-fermenter network and yield coefficients ($Y_{x/s,2}$, $Y_{x/p,2}$) are negligible.

In the co-fermentation system (model (*iii*)), λ is again the most influential parameter, explaining more than 50% of biomass concentration (*X*) variance throughout the time horizon; $\nu_{max,g}$ and $Y_{p/s,g}$ also contribute up to 30% of the variance (Fig. 5(c) and Table 5). Interaction effects are negligible, as compared to first order effects, which represent over the 90% uncertainty throughout almost the entire time horizon.

3.4. Product concentration

In model (*ii*), bioethanol concentration profiles (*P*) were analyzed starting at *t* = 10 h of the bioreactor network, because only in the second reactor bioethanol is produced. Bioethanol concentration for models (*i*) (Fig. 6(a)) and (*ii*) (Fig. 6(b)) is mainly influenced by first order effects of parameters explaining between 97% and 100% and 68% and 100%, respectively. In model (*i*), $Y_{x/p}$ is the main parameter followed by μ_{max} and K_s. These three parameters are influential through the entire bioethanol production period. The maximum specific growth rate of biomass μ_{max} is also influent through its interactions, with S^{int} between 21% and 28% (Table 6).

In model (*ii*), $Y_{x/p,2}$ is the main parameter throughout the entire batch time and explains between 30% and 40% of total variance of bioethanol concentration (Fig. 6(b) and Table 6). Also, K_s and $\mu_{max,2}$ are important, with decreasing influence at the end of the production process, together explaining between 49% and 10% of first order effects. In the case of $Y_{x/s,2}$, its influence increases along the time horizon. Additionally, $\mu_{max,1}$ and ν_{dead} have some influence

Table 6
Product concentration sensitivity indices.

	Model (*i*)						Model (*ii*)						Model (*iii*)											
	P						*P*						P_g						P_x					
	S_i			S_i^{int}			S_i			S_i^{int}			S_i			S_i^{int}			S_i			S_i^{int}		
	t = 2	*t* = 5	*t* = 25	*t* = 2	*t* = 5	*t* = 25	*t* = 15	*t* = 25	*t* = 35	*t* = 15	*t* = 25	*t* = 35	*t* = 1	*t* = 2	*t* = 5	*t* = 1	*t* = 2	*t* = 5	*t* = 1	*t* = 2	*t* = 5	*t* = 1	*t* = 2	*t* = 5
$Y_{x/s}$	0.02	0.02	0.03	0.02	0.02	0.05	0.05	0.13	**0.22**	0.14	0.14	0.13	0.01	**0.57**	**0.57**				0.01	0.02	0.04	**1.1**	**1.0**	**1.3**
$Y_{x/p}$	**0.43**	**0.43**	**0.44**				**0.29**	**0.36**	**0.36**	0.07	0.10	0.13				0.13	0.13		0.01	0.01	0.09	**1.1**	**1.0**	**1.2**
μ_{max}	**0.30**	**0.31**	**0.26**	**0.28**	**0.27**	**0.21**	0.12	0.02		**0.23**	**0.32**	**0.38**				0.13	0.13					**1.3**	**1.2**	**1.6**
K_s	**0.21**	**0.21**	**0.18**				**0.25**	**0.18**	0.06	**0.25**	**0.34**	**0.39**				0.13	0.13	0.01	0.01	0.02	0.02	**1.1**	**1.0**	**1.3**
v_{dead}	0.03	0.03	0.06	0.01			**0.21**	0.13	0.04	0.06	0.14	**0.22**	**0.65**			0.05	0.13	0.13	0.01	0.03	0.03	**1.1**	**1.0**	**1.3**
							0.06	0.04		0.13	**0.18**	**0.25**					0.13	0.13	**0.77**	**0.66**	**0.56**			**0.2**
													0.08	**0.39**	**0.39**		0.3	0.3	0.05	0.08	0.17	**1.2**	**1.1**	**1.2**
Σ	0.99	1.00	0.97				0.98	0.86	0.68				0.74	0.96	0.96				0.86	0.82	0.91			

Sub-index 1, 2, *g* and *x* stands for biomass production bioreactor, ethanol production bioreactor, glucose and xylose respectively. S_i and S_i^{int} represent first order and interactional sensitivity indices for parameter *i*. *t*: time (h). The highest values obtained are marked in bold.

at the beginning of the fermentation stage. Interaction effects become important in the last part of bioethanol production process, after time *t* = 10 h (Table 6), being $\mu_{max,1}$ and $\mu_{max,2}$ the most influential parameters, which together have S^{int} between 0.50 and 0.80 in bioethanol concentration.

In model (*iii*), bioethanol concentration is represented by two differential state variables, P_g (Fig. 6(c)) and P_x (Fig. 6(d)), that correspond to bioethanol produced from glucose and xylose concentrations, respectively. The model captures the high bioethanol production rate during the initial phase of primarily glucose fermentation, followed by the slower rate from xylose after glucose is consumed. The simultaneous utilization of both substrates is also predicted by the model. Up to glucose depletion (around *t* = 1.5 h), the maximum specific rate of ethanol production from glucose, $v_{max,g}$, is the most important parameter for first order effects, explaining over 75% of total variance (Fig. 6(c) and Table 6); and it is influential through its interactions (S^{int} = 0.13). When glucose is depleted, both $Y_{p/s,g}$ and λ together explain the 96% of the bioethanol from glucose concentration (P_g) variance due to first order effects. For bioethanol produced from xylose concentration (P_x), S_i profile shows that first order effects explain around 70% of the total variance for P_x concentration being $v_{max,x}$ the most influential parameter, explaining from 77% to 56% of ethanol from xylose concentration variance along the time horizon. As it can be seen in Fig. 6(d), S_i concentration profiles for bioethanol produced from xylose are smoother than from glucose, which is in line with slower xylose conversion.

4. Conclusions

Parametric dynamic GSA was carried out on bioreactor models of increasing complexity for bioethanol production. Time profiles for sensitivity indices related to each parameter, allowed the identification of model parameters that were more influential on model variables. In model (*i*) μ_{max} and K_s were the most influential parameters, followed by v_{dead} and $Y_{x/s}$. In model (*ii*), the parameter with largest contribution to model variables uncertainty was $\mu_{max,1}$, both through first order effects and interactions with other parameters. In model (*iii*), the most influential parameter over all model variables was λ, due to its first order effects and interactions.

Acknowledgments

Financial support from the National Research Council CONICET (Argentina) under Grant PIP 2011 11220110101078 and Universidad Nacional del Sur (Argentina) under Grant PGI 24/M125 is gratefully acknowledged.

References

Albernas-Carvajal, Y., Corsano, G., Kafarov, V.V., González Cortés, M., González Suárez, E., 2014. Optimal design of pre-fermentation and fermentation stages applying nonlinear programming. Energy Convers. Manage. 87, 1195–1201.
Chen, M.L., Wang, F.S., 2010. Optimal trade-off design of integrated fermentation processes for ethanol production using genetically engineered yeast. Chem. Eng. J. 158 (2), 271–280.
Corsano, G., Aguirre, P.A., Iribarren, O., Montagna, J.M., 2004. Batch fermentation network model for optimal synthesis, design and operation. Ind. Eng. Chem. Res. 43, 4211–4219.
Corsano, G., Iribarren, O., Montagna, J.M., Aguirre, P.A., Suarez, E.G., 2006. Economic tradeoffs involved in the design of fermentation processes with environmental constraints. Chem. Eng. Res. Des. 84 (A10), 932–942.
Corsano, G., Vecchietti, A.R., Montagna, J.M., 2011. Optimal design for sustainable bioethanol supply chain considering detailed plant performance model. Comput. Chem. Eng. 35, 1384–1398.
Cukier, R., Fortuin, C., Shuler, K., Petschek, A., Schaibly, J., 1973. Study of the sensitivity of coupled reaction systems to uncertainties in rate coefficients. J. Chem. Phys. 59, 3873–3878.
Datta, R., Maher, M., Jones, C., Brinker, R., 2011. Ethanol – the primary renewable liquid fuel. J. Chem. Technol. Biotechnol. 86, 473–480.

Di Maggio, J., Diaz Ricci, J., Diaz, M., 2010. Global sensitivity analysis in dynamic metabolic networks. Comput. Chem. Eng. 34, 770–781.
Estrada, V., Diaz, M., 2010. Global sensitivity analysis in the development of first principle-based eutrophication models. Environ. Model. Software 25, 1539–1551.
Ho, N., Chen, Z., Brainard, A., 1998. Genetically engineered saccharomyces yeast capable of effective cofermentation of glucose and xylose. Appl. Environ. Microbiol. 64 (3), 1852–1859.
Homma, T., Saltelli, A., 1996. Importance measures in global sensitivity analysis of nonlinear models. Reliab. Eng. Syst. Saf. 52, 1–17.
Kent, E., Neumann, S., Kummer, U., Mendes, P., 2013. What can we learn from global sensitivity analysis of biochemical systems? PLoS ONE 8 (11), e79244. http://dx.doi.org/10.1371/journal.pone.0079244.
Krishnan, M., Ho, N., Tsao, G., 1999. Fermentation kinetics of ethanol production from glucose and xylose by recombinant *Saccharomyces* 1400 (pINH33). Appl. Biochem. Biotechnol. 78, 373–388.
Kucherenko, S., Delpuech, B., Iooss, B., Tarantola, S., 2015. Application of the control variate technique to estimation of total sensitivity indices. Reliab. Eng. Syst. Saf. 134, 251–259.
Leksawasdi, N., Joachimsthal, E.L., Rogers, P.L., 2001. Mathematical modeling of ethanol production from glucose/xylose mixtures by recombinant *Zymomonas mobilis*. Biotechnol. Lett. 23, 1087–1093.
Morales-Rodriguez, R., Meyer, A.S., Gernaey, K.V., Sin, G., 2011a. Dynamic model-based evaluation of processes configuration for integrated operation of hydrolysis and co-fermentation for bioethanol production from lignocellulose. Bioresour. Technol. 102, 1174–1184.
Morales-Rodriguez, R., Gernaey, K.V., Meyer, A.S., Sin, G., 2011b. A mathematical model for simultaneous saccharification and co-fermentation (SSCF) of C6 and C5 sugars. Chin. J. Chem. Eng. 19 (2), 185–191.
Moreno, M.S., Andersen, F., Diaz, M.S., 2013. Dynamic modeling and parameter estimation for unit operations in lignocellulosic bioethanol production. Ind. Eng. Chem. Res. 52, 4146–4160.
Morris, M., 1991. Factorial sampling plans for preliminary computational experiments. Technometrics 33, 161–174.
Muhaimin Samsudin, M., Mat Don, M., 2015. Assessment of bioethanol yield by S. cerevisiae grown on oil palm residues: Monte Carlo simulation and sensitivity analysis. Bioresour. Technol. 175, 417–423.
Nakamura, Y., Sawada, T., Inoue, E., 2001. Mathematical model for ethanol production from mixed sugars by *Pichia stipitis*. J. Chem. Technol. Biotechnol. 76, 586–592.
Nielsen, J., Villadsen, J., Lindén, G., 2003. Bioreaction Engineering Principles. Kluwer Academic/Plenum Publisher, New York.
Ochoa, M., Hoch, P., 2011. Global sensitivity analysis in bioreactor networks. Comput. Aided Chem. Eng. 29, 1436–1440.
PSEnterprise Ltd., 2014. gPROMS Model Developer Guide. Process Systems Enterprise Ltd, London.
Román-Martínez, A., Lanuza-Pérez, P., Cepeda-Rodriguez, M., 2014. Global sensitivity analysis for control of biological wastewater treatment. Comput. Aided Process Eng. 33, 709–714.
Romaní, A., Pereira, F., Johansson, B., Domingues, L., 2015. Metabolic engineering of Saccharomyces cerevisiae ethanol strains PE-2 and CAT-1 for efficient lignocellulosic fermentation. Bioresour. Technol. 179, 150–158.
Saltelli, A., Tarantola, S., 2002. On the relative importance of input factors in mathematical models: safety assessment for nuclear waste disposal. J. Am. Stat. Assoc. 97, 702–709.
Saltelli, A., Ratto, M., Andres, T., Campolongo, F., Cariboni, J., Gatelli, D., Saisana, M., Tarantola, S., 2008. Global Sensitivity Analysis. The Primer. John Wiley & Sons Ltd.
Savvopoulos, S., Misener, R., Panoskaltsis, N., Pistikopoulos, E.N., Mantalaris, A., 2015. Global sensitivity analysis for a model of B-cell chronic lymphocytic leukemia disease trajectories. Comput. Aided Chem. Eng. 37, 185–190.
Sharma, S., Rangaiah, G.P., 2013. Improved constraint handling technique for multi-objective optimization with application to two fermentation processes. In: Multi-Objective Optimization in Chemical Engineering: Developments and Applications. John Wiley & Sons, Ltd, pp. 129–156.
Sobol', I., 2001. Global sensitivity indices for nonlinear mathematical models and their Monte Carlo estimates. Math. Comput. Simul. 55, 271–280.
Sobol', I.M., 1993. Sensitivity estimates for nonlinear mathematical models. Math. Model. Comput. Exp. 1, 407–414.
Song, X., Zhang, J., Zhan, C., Xuan, Y., Ye, M., Xu, C., 2015. Global sensitivity analysis in hydrological modeling: review of concepts, methods, theoretical framework and applications. J. Hydrol. 523, 739–757.
Tang, Z., Zhenzhou, L., Zhiwen, L., Ningcong, X., 2015. Uncertainty analysis and global sensitivity analysis of techno-economic assessments for biodiesel production. Bioresour. Technol. 175, 502–508.
Todri, E., Amenaghawon, A., Jimenez del Val, I., Leak, D., Kontoravdi, C., Kucherenko, S., Shah, N., 2014. Global sensitivity analysis and meta-modeling of an ethanol production process. Chem. Eng. Sci., 114–127